DALTON
FULL PAPER

The solution thermolysis approach to molybdenum(V) alkoxides: synthesis, solid state and solution structures of the bimetallic alkoxides of molybdenum(V) and niobium(V), tantalum(V) and tungsten(VI)

Anders Johansson,[a] Magnus Roman,[a] Gulaim A. Seisenbaeva,[b] Lars Kloo,[c] Zoltan Szabo[c] and Vadim G. Kessler[a]*

[a] *Department of Chemistry, Swedish University of Agricultural Sciences, Box 7015, 75007 Uppsala, Sweden*
[b] *Moscow State Academy of Fine Chemical Technology, Pr. Vernadskogo 86, 117571 Moscow, Russia*
[c] *Inorganic Chemistry, Royal University of Technology, 100 44 Stockholm, Sweden*

Received 24th September 1999, Accepted 14th December 1999

No complex formation can be observed between molybdenum(VI) oxoalkoxides and the alkoxides of niobium(V) or tantalum(V) at room temperature. The bimetallic derivatives of molybdenum(V), $Mo_4M_2O_8(O^iPr)_{14}$, where M = Nb **1** and Ta **2**, were instead isolated on cooling from the solutions of the isopropoxides in toluene subjected to a short-time reflux. The X-ray single crystal study showed both **1** and **2** to be built of $(^iPrO)_3M(\mu\text{-}O^iPr)_3MoO(\mu\text{-}O)_2MoO(\mu\text{-}O^iPr)_2MoO(\mu\text{-}O)_2MoO(\mu\text{-}O^iPr)_3M(O^iPr)_3$ non-linear chain molecules with 2 Mo–Mo bonds (2.5836(8) Å) and short but non-bonding Mo–M distances (3.1791(8) Å for **1** and 3.1746(8) Å for **2**). According to NMR and EXAFS data this structure becomes very fluxional or might even be partially broken into homometallic components in hydrocarbon solutions. The oxidation of **2** with traces of oxygen leads to the formation of $Mo_3Ta_2O_8(O^iPr)_{10}$ **3**. Compound **3** can be isolated in a pure form from the reaction of $MoO(O^iPr)_4$ with $Ta(O^iPr)_4(OMe)$ **6**: the presence of methoxide ligands leads to the formation of additional oxoligands *via* non-reductive thermolysis leading to the formation of a $(CH_3)_2C(OMe)_2$ ketal as organic byproduct. The molecules of **3** are 5-member rings with a $MoO(\mu\text{-}O)_2$-MoO fragment in the basis (Mo–Mo 2.5730(13) Å), coupled to two $(\mu\text{-}O^iPr)_2Ta(O^iPr)_3$ fragments that are joined together by an oxomolybdate ligand $(\mu\text{-}O)_2MoO_2$. According to NMR-spectroscopic data the aggregate is preserved and rigid in solution. $Mo_4Ta_4O_{16}(O^iPr)_{12}$ **4** was found to be one of the products of complete oxidation of **2** (and **3**) on prolonged contact with dry oxygen. The thermal treatment of the solutions of $MoO(O^iPr)_4$ and $WO(O^iPr)_4$ in toluene yields $Mo^V{}_4O_8(Mo,W)^{VI}{}_2O_2(O^iPr)_{12}$ **5** with a molecular structure very close to its homometallic analog $Mo_6O_{10}(O^iPr)_{12}$. The complete X-ray single crystal study was carried out for the sample of **5** with $Mo^V{}_4O_8(Mo_{0.45}W_{0.55})^{VI}{}_2O_2(O^iPr)_{12}$ composition.

The information present in the literature on the synthesis and molecular structures of molybdenum(V) alkoxides is rather limited. No homoleptic derivatives have been reported. Common approaches such as alcoholysis of halides, *e.g.* $MoCl_5$, have provided access to oxoalkoxide halides as $Mo_2O_2(\mu\text{-}OEt)_2(\mu\text{-}EtOH)Cl_4$[1] or, in the presence of amines, to oxoalkoxides as $MoO(OMe)_3$[2] (the latter have been characterized only by microanalysis). The same reaction in the presence of $Mg(OMe)_2$ as a base gave a bimetallic Mg–Mo oxoalkoxide—$Mg_2Mo^V{}_2O_2(OMe)_{10}(MeOH)_4$.[3] The electrochemical reduction of molybdenum(VI) alkoxides in the presence of LiCl as conductive additive yielded bimetallic Li–Mo oxoalkoxides such as $LiMo_2O_2(OMe)_7(MeOH)$[4] and $LiMo_2O_2(OEt)_7$.[5] The oxidation of molybdenum alkoxide derivatives in lower oxidation states were reported to provide a route to Mo(V) alkoxide halides, $Mo(OR)_3X_2$, where R = ^{i}Pr, Ph, X = Cl, Br, I, *via* the reaction of $Mo_2(OR)_6$ with halogenes;[6] and to a mixed-valence oxoalkoxide complex $Mo_6O_{10}(O^iPr)_{12}$ *via* the reaction of Mo(III) isopropoxide with molecular oxygen.[7] The solvolysis of the latter oxoalkoxide complex in the presence of pyridine gave a pyridine solvate of Mo(V) dioxoisopropoxide—$[MoO_2(O^iPr)(py)]_4$.[7] We have recently reported the formation of $Mo_6O_{10}(O^iPr)_{12}$ on spontaneous decomposition of $MoO(O^iPr)_4$ (on storage even at room temperature).[8] The easy formation of this derivative, its peculiar structure [its molecules are non-linear chains with a Mo(V) core—$MoO(\mu\text{-}O)_2MoO(\mu\text{-}O^iPr)_2MoO(\mu\text{-}O)_2MoO$, containing two Mo–Mo single bonds, capped by two Mo(VI) ligands—$(\mu\text{-}O^iPr)_2MoO(O^iPr)_3$] and the definite mobility of the latter in solution being responsible for the easy solvolysis gave us an idea to investigate the possibility to prepare bimetallic alkoxides of molybdenum with high-valent elements such as niobium, tantalum or tungsten *via* exchange of the alkoxomolybdate(VI) ligands for the other alkoxometallate ones in this structure.

Experimental

All the manipulations were carried out in a dry nitrogen atmosphere using the Schlenk technique or a dry box. The alcohols were purified by distillation over $Al(O^iPr)_3$ or $Mg(OMe)_2$ under argon. IR spectra of nujol mulls were registered with a Bruker IFS-55 spectrometer. The ^{1}H NMR spectra were obtained with a Varian 400 MHz spectrometer, ^{13}C and ^{17}O (natural abundance referred to ^{17}O-enriched water) NMR spectra—with Bruker DMX 500 MHz, using dry deaerated toluene as solvent (using TMS as internal and 20 vol% solution of $CDCl_3$ as external standards). The metal ratio in the samples was determined, exploiting the facilities of Arrhenius Laboratory,

Stockholm University, Sweden, on JEOL-820 scanning electron microscope (SEM), supplied with Link AN-10000 energy dispersive spectrometer (EDS).

Synthesis and isolation of the products obtained

The starting reagents used in this work [$MoO(OMe)_4$, $WO(OMe)_4$,[4] $Ta(OMe)_5$, $Ta_2O(O^iPr)_8(^iPrOH)$, $Ta(O^iPr)_5$,[9] and $Nb(O^iPr)_5$[10]] were prepared by anodic oxidation of metals in alcohols and purified according to conventional techniques. Alcohol interchange reactions with isopropanol were used to obtain $MoO(O^iPr)_4$ and $WO(O^iPr)_4$ and were performed by triply repeated dissolution of a measured quantity of methoxide (0.5–0.7 g) in excess of ^iPrOH (10 ml for each treatment) with subsequent evaporation to dryness.

$[Mo_4Nb_2O_8(O^iPr)_{14}]$ 1. $Nb(O^iPr)_5$ (0.968 g, 2.49 mmol) and $MoO(O^iPr)_4$ (2.314 g, 6.65 mmol) were dissolved in 5 ml toluene. The yellow solution obtained was heated under reflux for half an hour. Its color turned into orange and then into orange-brown and its viscosity increased noticeably. The solution was left for crystallization at 0 °C for 3 days. The brownish orange needles formed were isolated by decantation, washed with 1 ml toluene and dried *in vacuo* at room temperature. Yield 2.732 g {72% in relation to $Nb(O^iPr)_5$}. IR/cm^{-1}: 1344m, 1329m, 1173s, 1155 (sh), 1119s, 1108 (sh), 1027m, 1000s, 982vs, 952s, 943s, 916m, 855m, 831m, 815m, 754m, 650w, 603s, 583s, 569s, 542m, 461s, 443s. NMR ^{1}H/ppm: 5.40 septet (7H, C*H*), 2.06 doublet (42H, CH_3) at 303 K and 5.05 (4H, C*H*), 4.73 (2H, C*H*), 4.63 (1H, C*H*), 1.24 (very broad 42H, CH_3) at 223 K.

$[Mo_4Ta_2O_8(O^iPr)_{14}]$ 2. *Method A*. $Ta(O^iPr)_5$ (0.905 g, 1.89 mmol) and $MoO(O^iPr)_4$ (1.514 g, 4.35 mmol) were dissolved in 5 ml toluene. The light yellow solution obtained was heated under reflux turning first greenish yellow and then dark orange. The heating was stopped after 30 min and the dark orange solution formed was left for crystallization overnight at 0 °C. The bright orange thin plates formed were isolated by decantation, washed with 1 ml toluene and dried *in vacuo* at room temperature. Yield 2.773 g (86% in relation to $Ta(O^iPr)_5$). *Method B*. The amorphous powder of $Ta_2O(O^iPr)_8$ (0.452 g, 0.53 mmol), obtained by prolonged drying of $Ta_2O(O^iPr)_8(^iPrOH)$ *in vacuo* at room temperature was mixed with solution of $MoO(O^iPr)_4$ (0.724 g, 2.08 mmol) in 3 ml toluene. The greenish yellow solution obtained was refluxed under 15 min and left for crystallization overnight at 0 °C. The product was isolated by decantation, washed with 0.5 ml toluene and dried *in vacuo* at room temperature. Yield 0.836 g {92% in relation to $Ta_2O(O^iPr)_8$}. IR/cm^{-1}: 1466s, 1450s, 1417m, 1381s, 1369s, 1173m, 1160m, 1130s, 1119s, 1024s, 1002s, 979s, 948s, 912m, 824s, 808m, 574m, 542m, 463m. NMR ^{1}H/ppm: 5.33 septet (7H, C*H*), 1.96 doublet (42H, CH_3) at 303 K and 4.85 (4H, C*H*), 4.36 (3H, C*H*), 1.20 (very broad 42H, CH_3) at 223 K and 5.15 (1H, C*H*), 5.05 (3H, C*H*), 4.54 (3H, C*H*), 1.22 (very broad 42H, CH_3) at 217 K; ^{13}C/ppm: 63.59 (*C*H), 25.10 (*C*H_3) at 303 K.

$[Mo_3Ta_2O_8(O^iPr)_{10}]$ 3. $Ta(OMe)_5$, (0.555 g, 1.65 mmol) were dissolved in 10 ml isopropanol, warmed up to 40 °C and then evaporated to dryness at room temperature. This operation was repeated three times. The product (having the approximate composition $Ta(O^iPr)_4(OMe)$ according to ^{1}H NMR spectra) was mixed with $MoO(O^iPr)_4$ (0.943 g, 4.00 mmol) in 3 ml toluene and the yellow solution obtained was subjected to reflux for 1 h. Its color then changed to bright orange. Subsequent cooling (even to −30 °C) gave only a few flaky polycrystals. The reaction mixture was then evaporated to dryness, dissolved in 3 ml of hexane and left for crystallization overnight at −30 °C. The product—large rectangular prisms were isolated by decantation, washed with 0.5 ml hexane and dried *in vacuo* at room temperature. Yield 0.306 g {27% in relation to $Ta(OMe)_5$}. IR/cm^{-1}: 1466s, 1448s, 1374s br, 1196m, 1169m, 1151w, 1124s, 1106m, 1038s, 1013s, 1000m, 988m, 977m, 952m, 939m, 925m, 909s, 889m, 873m, 849m, 826s, 819s, 810s, 754m, 736s, 605s, 578m, 558m, 547m, 533m, 477s, 454s, 432m. NMR ^{1}H/ppm: 5.69 septet (6H, C*H*), 5.48 septet (4 H, C*H*) (3 : 2), 1.82 doublet (36H, CH_3) and 1.67 doublet (24H, CH_3), ^{13}C/ppm: 76.81, 74.85, 74.27 (*C*H), 25.19, 25.00, 24.87, 24.81 (*C*H_3), ^{17}O/ppm: 872.8, 880.3, 895.5, 903.6, 578, 552, 46.

$[Mo_4Ta_4O_{16}(O^iPr)_{12}]$ 4. $MoO(O^iPr)_4$ (0.472 g, 1.36 mmol) and $Ta(O^iPr)_5$ (0.674g, 1.41 mmol) were dissolved in 5 ml of toluene and the bright yellow solution obtained was subjected to reflux for 30 min. The brownish orange viscous liquid thus formed was left for two weeks in a flask covered by a serum cup at room temperature. Its color then slowly changed to light brown. The solvent was evaporated *in vacuo* and the light-brown glassy residue redissolved in 3 ml of hexane and left for crystallization overnight. The colorless transparent crystals formed were separated by filtration and dried *in vacuo*. Yield 0.127 g (18%). IR/cm^{-1}: 1381m, 1367m, 1337w, 1262w, 1179s, 1168m, 1120s br, 1007s br, 966w, 904 (sh), 877s, 840s, 810s br, 684 (sh), 583s br, 565 (sh), 455m br. NMR ^{1}H/ppm: 5.28 septet (1H, C*H*), 1.56 doublet (6H, CH_3) at 303 K and 3.97 (broad 1H, C*H*), 1.21 (broad 6H, CH_3) at 223 K.

$[Mo^V_4O_8(Mo_{0.45}W_{0.55})^{VI}_2O_2(O^iPr)_{12}]$ 5. $WO(O^iPr)_4$ (0.863 g, 1.98 mmol) was added to a solution of $MoO(O^iPr)_4$ (1.399 g, 4.02 mmol) in 5 ml toluene. The resulting light yellow solution was subjected to reflux for 30 min. Its color changed to a yellowish brown and its viscosity increased. It was left for crystallization at room temperature (as no crystallization could be observed for this system at lowered temperatures) that resulted in formation of yellowish brown thick needles that were isolated by decantation, washed with 1 ml toluene and dried *in vacuo*. Yield 1.137 g {41% in relation to $WO(O^iPr)_4$}. IR/cm^{-1}: 1471s, 1457s, 1448s, 1374s br, 1360m, 1349w, 1324m, 1169m, 1137s, 1126s, 1115s, 1099s br, 1011w, 984s, 970s, 959s sharp, 932s, 912s, 853m, 833m, 810w, 646m, 616s br, 569w, 499m, 486s, 465m. NMR ^{1}H/ppm: 5.82, 5.64, 4.90, 1.98, 1.80, 1.54, 1.30 all very broad and not resolved at 303 K and 4.48, 4.33, 4.16, 3.98, 1.28 very broad and not resolved at 223 K.

$Ta_2(OMe)_2(O^iPr)_8$ 6. The solution prepared in the same way as for the synthesis of **3** (a portion of $Ta(OMe)_5$ (0.716 g, 2.1 mmol) was treated three times with 10 ml portions of ^iPrOH with evacuation after the addition of each portion. The white crystalline product thus obtained was mixed with $MoO(O^iPr)_4$ (1.392 g, 4.0 mmol) in 20 ml of toluene and was not subjected to thermal treatment but left for several weeks at −30 °C in the refrigerator. Several colorless single crystals identified as **6** by the X-ray single crystal study were formed along with the needle-shaped yellow crystals of $MoO(O^iPr)_4$.

Crystallography

All compounds studied are extremely sensitive to ambient atmosphere and were therefore placed into glass capillaries, sealed under vacuum, for data collection. The crystal data and the experimental conditions are shown in Table 1. The data were collected using SMART CCD 1K diffractometer at 22 °C. All calculations were performed on an IBM PC using the SHELXTL program package[11] Version 5.3. All structures were solved by direct methods. The positions of all non-hydrogen atoms in the structures **1** (normal temperature modification), **2**, **5** and **6** were refined by the full matrix least squares technique (the occupancy factors for the position W(1) in **5** occupied by both Mo and W atoms were refined in supposition of their sum being equal to 1.0. The values obtained were in agreement with those obtained by EDS-analysis within experimental errors).

Table 1 Crystal data and the details of diffraction experiments for compounds **1**, **2**, **3** and **5**

	1	**2**	**3**	**5**	**6**
Chemical formula	$C_{42}H_{98}Mo_4Nb_2O_{22}$	$C_{42}H_{98}Mo_4Ta_2O_{22}$	$C_{30}H_{70}Mo_3O_{18}Ta_2$	$C_{36}H_{84}Mo_{4.96}O_{22}W_{1.04}$	$C_{26}H_{62}O_{10}Ta_2$
Formula weight	1524.78	1700.86	1368.58	1620.49	896.66
Crystal system	Triclinic	Triclinic	Orthorhombic	Triclinic	Triclinic
Space group	$P\bar{1}$	$P\bar{1}$	*Pbca*	$P\bar{1}$	$P\bar{1}$
μ/mm^{-1}	1.139	4.091	5.079	3.184	5.662
*R*1	0.0453	0.0430	0.0507	0.0641	0.0422
*wR*2	0.1030	0.0943	0.1161	0.1489	0.0820
a/Å	10.0293(12)	10.0444(17)	18.8123(11)	10.00(2)[a]	9.137(2)
b/Å	10.9976(13)	11.0070(19)	18.5541(11)	11.44(2)[a]	9.865(2)
c/Å	15.7176(18)	15.769(3)	29.0517(18)	13.29(3)[a]	12.474(3)
α/°	94.154(2)	94.159(5)		98.95(4)	111.551(4)
β/°	93.941(2)	94.091(7)		91.64(4)	98.789(4)
γ/°	107.329(2)	107.143(4)		106.15(4)	104.757(4)
V/Å^3	1643.1(3)	1653.7(5)	10140.4(11)	1439(5)	972.5(4)
T/K	295(2)	295(2)	295(2)	295(2)	295(2)
Z	1	1	8	1	1
Number of independent reflections	7114 [*R*(int) = 0.0315]	7141 [*R*(int) = 0.0348]	11928 [*R*(int) = 0.0677]	3526 [*R*(int) = 0.0442]	3347 [*R*(int) = 0.0309]
Number of observed reflections	3116 [$I \geq 2\sigma(I)$]	3909 [$I \geq 2\sigma(I)$]	5189 [$I \geq 2\sigma(I)$]	1761 [$I \geq 2\sigma(I)$]	3347 [$I \geq 2\sigma(I)$]

[a] Strikingly high standard deviations for the unit cell parameters originate supposedly from the disorder of domains (that might have different chemical composition).

The positions of the hydrogen atoms in these structures were calculated geometrically and included into the final refinement in isotropic approximation; the thermal parameters for H-atoms were taken as $U_{iso} = 1.50U_{eq}(C)$, where $U_{eq}(C)$ was the equivalent parameter for the carbon atom to which the hydrogen atom is attached.

The solution of the structure of **3** by direct methods provided the coordinates of two tantalum and three molybdenum atoms. The subsequent Fourier syntheses have revealed the positions of all other non-hydrogen atoms and also that of Mo(3A)—the position alternative to Mo(3) in the disorder of the MoO_2-fragment in the structure. The analysis of the valent angles at Mo-atoms permitted the identification of the disordered fragments as Mo(3)O(17A)O(18A) and Mo(3A)O(17)O(18). The SOF-parameters were refined by the supposition that one value was the same for Mo(3), O(17A) and O(18A) on one hand, and the other for Mo(3A), O(17) and O(18), the sum of these two being equal to 1.0 as they described the disorder of one MoO_2-fragment. In the structure of **3** it was possible to refine in the anisotropic approximation the positions of all non-hydrogen atoms except the carbon atoms belonging to two isopropyl radicals (C(12), C(25), C(26) and C(23), C(27), C(28)) severely disordered due to thermal motion. We were not able to resolve the disorder at room temperature and as we did not possess the equipment for low-temperature experiments, we included the positions of these atoms into the final refinement using the isotropic approximation. No attempts have been made to locate the positions of the hydrogen atoms in the structure of **3**.

We have observed the formation of a low-temperature modification of **1** stable below 4 °C. It was this modification we observed to form on crystallization under the conditions described for the crystallization of **1** in the synthetic procedures. The single crystals of this modification transformed spontaneously into the single crystals of the normal temperature phase in approximately 2 h at 22 °C. The incomplete data collection run under 40 min with the total exposure time 2 s/frame, 1448 independent reflections observed, permitted the determination of the unit cell parameters (triclinic, $P\bar{1}$, $a = 10.207(6)$, $b = 10.988(7)$, $c = 17.767(9)$ Å, $\alpha = 77.59(2)$, $\beta = 84.00(2)$, $\gamma = 68.07(2)°$) and obtaining a model of the structure. In the latter all the positions of metal and oxygen atoms could be located and refined anisotropically, but the difference Fourier syntheses unfortunately allowed the localization of only 14 of 21 symmetrically independent carbon atoms. The final discrepancy factors were $R1 = 0.1182$, $wR2 = 0.3174$.

The details of the X-ray single crystal study of **4** (tetragonal, I-4, $a = b = 14.998(6)$, $c = 14.974(8)$ Å) will be published elsewhere.[5]

CCDC reference number 186/1778.

See http://www.rsc.org/suppdata/dt/a9/a907720k/ for crystallographic files in .cif format.

EXAFS spectroscopy

X-Ray absorption data for compound **2** were recorded at beamline 4-1 at the Stanford Synchrotron Radiation Laboratory (SSRL) operating at 3.0 keV and 85–90 mA. Monochromatic radiation was obtained from an Si(220) double-crystal monochromator. High-order harmonics were rejected by 50% detuning. Incident and transmitted X-rays were monitored with nitrogen- and argon-filled ion chambers. Fluorescence was recorded by a Lytle detector filled with Kr gas. Five scans were made for the Mo K-edge (referenced internally to Mo foil at 20004 eV) and for the Ta L_3-edge (referenced internally to Ta foil at 9881 eV) for both solid and liquid samples. The liquid samples were contained in 1 mm thick cells with Kapton film as windows. The data were processed by standard procedures for pre-edge subtraction, spline fit and removal.[12]

Results and discussion

Molecular and crystal structures

The structures of compounds **1** (normal temperature modification, Fig. 1, Table 2) and **2** (Fig. 2, Table 3) are very similar, which is rather typical for the analogous derivatives of Nb and Ta,[9] and also to that of the compound **5** (Fig. 3, Table 4). They are built up of non-linear centrosymmetric chain molecules, where the central $MoO(\mu\text{-}O)_2MoO(\mu\text{-}O^iPr)_2MoO(\mu\text{-}O)_2MoO$ zigzag core practically has almost the same shape and size as that in the homometallic prototype $Mo_6O_{10}(O^iPr)_{12}$.[7] The most important parameters such as the Mo(1)–Mo(2) distances (2.5837(8) Å in **1**, 2.5836(9) Å in **2**, to be compared with 2.581(4) Å in **4**, indicating the presence of single Mo–Mo bonds), Mo(1)–M(1) (3.1791(8) Å for M = Nb **1** and 3.1746(8) Å for M = Ta **2**) and the Mo(2)–Mo(1)–M(1) angles (136.12(3) and 136.62(3)° in **1** and **2** respectively) are in fact similar if not always coinciding within the standard deviations for the experimental values. The distances for the Mo=O double bonds

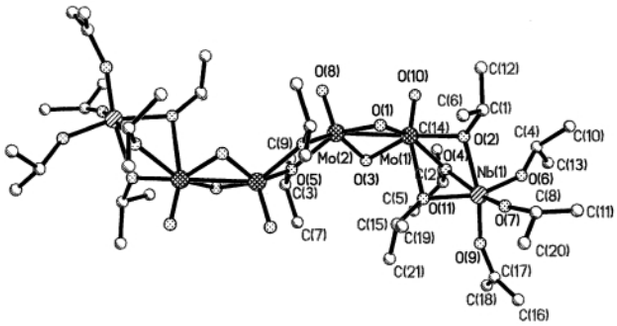

Fig. 1 The molecular structure of $Mo_4Nb_2O_8(O^iPr)_{14}$ **1**.

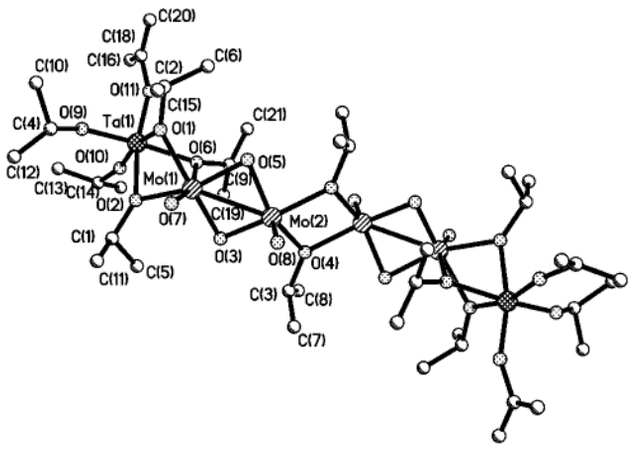

Fig. 2 The molecular structure of $Mo_4Ta_2O_8(O^iPr)_{14}$ **2**.

Table 2 Selected bond lengths (Å) and angles (°) for compound **1**

Mo(1)–O(10)	1.666(4)	Nb(1)–O(7)	1.836(4)
Mo(1)–O(1)	1.926(4)	Nb(1)–O(9)	1.846(5)
Mo(1)–O(3)	1.930(4)	Nb(1)–O(6)	1.867(4)
Mo(1)–O(4)	2.081(4)	Nb(1)–O(11)	1.989(4)
Mo(1)–O(2)	2.088(3)	Nb(1)–O(2)	2.139(4)
Mo(1)–O(11)	2.448(4)	Nb(1)–O(4)	2.141(4)
Mo(1)–Mo(2)	2.5837(8)	O(2)–C(1)	1.451(6)
Mo(1)–Nb(1)	3.1791(8)	O(4)–C(2)	1.429(7)
Mo(2)–O(8)	1.671(4)	O(5)–C(3)	1.465(7)
Mo(2)–O(1)	1.910(4)	O(6)–C(4)	1.405(8)
Mo(2)–O(3)	1.918(4)	O(7)–C(8)	1.445(9)
Mo(2)–O(5)#1	2.061(4)	O(9)–C(17)	1.385(10)
Mo(2)–O(5)	2.081(4)	O(11)–C(15)	1.408(9)
O(5)–Mo(2)#1	2.061(4)		
Mo(2)–Mo(1)–Nb(1)	136.12(3)	O(7)–Nb(1)–O(9)	99.6(2)
O(10)–Mo(1)–O(1)	108.18(19)	O(7)–Nb(1)–O(6)	97.23(19)
O(10)–Mo(1)–O(3)	106.69(18)	O(9)–Nb(1)–O(6)	96.3(2)
O(1)–Mo(1)–O(3)	91.30(15)	O(7)–Nb(1)–O(11)	98.54(18)
O(10)–Mo(1)–O(4)	99.50(19)	O(9)–Nb(1)–O(11)	95.66(18)
O(1)–Mo(1)–O(4)	150.31(16)	O(6)–Nb(1)–O(11)	158.28(18)
O(3)–Mo(1)–O(4)	90.87(15)	O(7)–Nb(1)–O(2)	93.65(18)
O(10)–Mo(1)–O(2)	98.11(17)	O(9)–Nb(1)–O(2)	165.05(17)
O(1)–Mo(1)–O(2)	92.67(15)	O(6)–Nb(1)–O(2)	88.79(17)
O(3)–Mo(1)–O(2)	152.24(16)	O(11)–Nb(1)–O(2)	75.42(16)
O(8)–Mo(2)–O(1)	109.23(18)	O(7)–Nb(1)–O(4)	163.81(18)
O(8)–Mo(2)–O(3)	111.53(19)	C(1)–O(2)–Mo(1)	132.1(4)
O(1)–Mo(2)–O(3)	92.18(15)	C(1)–O(2)–Nb(1)	128.3(4)
O(8)–Mo(2)–O(5)#1	108.23(19)	C(2)–O(4)–Mo(1)	132.2(4)
O(1)–Mo(2)–O(5)#1	86.37(15)	C(2)–O(4)–Nb(1)	126.7(4)
O(3)–Mo(2)–O(5)#1	138.27(16)	Mo(1)–O(4)–Nb(1)	97.71(15)
O(8)–Mo(2)–O(5)	104.16(18)	Mo(2)#1–O(5)–Mo(2)	108.76(16)
O(1)–Mo(2)–O(5)	144.27(15)	C(4)–O(6)–Nb(1)	148.3(4)
Mo(1)–Mo(2)–Nb(1)	97.52(15)	C(8)–O(7)–Nb(1)	165.6(5)
Mo(2)–Mo(3)–Nb(1)	84.37(14)	C(17)–O(9)–Nb(1)	160.2(7)

Symmetry transformations used to generate equivalent atoms: #1 $-x+1, -y, -z+1$.

(Mo(1)–O(10) 1.666(4), Mo(2)–O(8) 1.671(4) Å in **1** and Mo(1)–O(7) 1.680(5), Mo(2)–O(8) 1.673(5) Å in **2**, and Mo(1)–O(9) 1.661(12), Mo(2)–O(11) 1.654(10) Å in **5**), the nearly

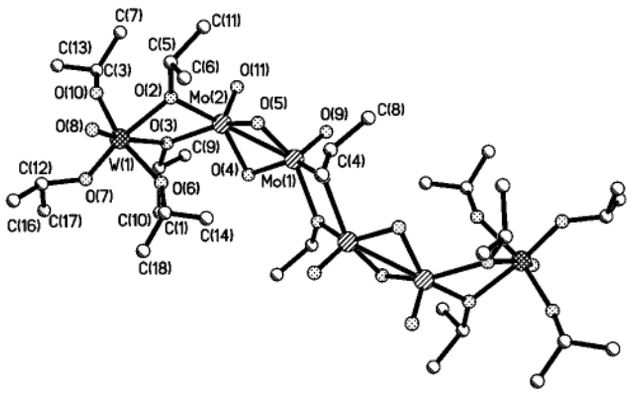

Fig. 3 The molecular structure of $Mo_4(Mo,W)_2O_{10}(O^iPr)_{12}$ **5**.

Table 3 Selected bond lengths (Å) and angles (°) for compound **2**

Mo(1)–O(7)	1.680(5)	Ta(1)–O(11)	1.847(6)
Mo(1)–O(5)	1.923(4)	Ta(1)–O(10)	1.859(5)
Mo(1)–O(3)	1.923(4)	Ta(1)–O(9)	1.873(5)
Mo(1)–O(1)	2.078(4)	Ta(1)–O(6)	2.002(5)
Mo(1)–O(2)	2.099(4)	Ta(1)–O(2)	2.133(5)
Mo(1)–O(6)	2.443(4)	Ta(1)–O(1)	2.136(4)
Mo(1)–Mo(2)	2.5836(9)	Ta(1)–Mo(1)	3.1746(8)
Mo(2)–O(8)	1.673(5)	O(1)–C(2)	1.450(8)
Mo(2)–O(5)	1.909(4)	O(2)–C(1)	1.448(8)
Mo(2)–O(3)	1.926(4)	O(4)–C(3)	1.474(8)
Mo(2)–O(4)	2.067(5)	O(6)–C(9)	1.404(12)
Mo(2)–O(4)#1	2.085(5)	O(9)–C(4)	1.421(10)
O(4)–Mo(2)#1	2.085(5)	O(10)–C(14)	1.426(11)
Mo(2)–Mo(1)–Ta(1)	136.62(3)	O(11)–Ta(1)–O(10)	99.1(3)
O(7)–Mo(1)–O(5)	107.3(2)	O(11)–Ta(1)–O(9)	96.0(2)
O(7)–Mo(1)–O(3)	107.6(2)	O(10)–Ta(1)–O(9)	95.8(2)
O(5)–Mo(1)–O(3)	91.72(18)	O(11)–Ta(1)–O(6)	94.6(2)
O(7)–Mo(1)–O(1)	98.9(2)	O(10)–Ta(1)–O(6)	98.7(2)
O(5)–Mo(1)–O(1)	91.50(18)	O(9)–Ta(1)–O(6)	160.4(2)
O(3)–Mo(1)–O(1)	151.0(2)	O(11)–Ta(1)–O(2)	164.7(2)
O(7)–Mo(1)–O(2)	96.8(2)	O(10)–Ta(1)–O(2)	94.3(2)
O(5)–Mo(1)–O(2)	152.8(2)	O(9)–Ta(1)–O(2)	89.8(2)
O(3)–Mo(1)–O(2)	92.77(17)	O(6)–Ta(1)–O(2)	76.0(2)
O(1)–Mo(1)–O(2)	72.16(17)	O(11)–Ta(1)–O(1)	95.7(2)
O(7)–Mo(1)–O(6)	161.5(2)	O(10)–Ta(1)–O(1)	164.4(2)
O(5)–Mo(1)–O(6)	86.02(19)	O(9)–Ta(1)–O(1)	87.5(2)
O(8)–Mo(2)–O(5)	111.3(2)	O(6)–Ta(1)–O(1)	75.13(18)
O(8)–Mo(2)–O(3)	109.1(2)	O(2)–Ta(1)–O(1)	70.35(17)
O(5)–Mo(2)–O(3)	92.07(18)	Mo(1)–O(2)–Ta(1)	97.20(18)
O(8)–Mo(2)–O(4)	108.3(2)	Ta(1)–O(6)–Mo(1)	90.61(19)
O(5)–Mo(2)–O(4)	138.5(2)	C(2)–O(1)–Mo(1)	131.7(4)
O(3)–Mo(2)–O(4)	86.48(18)	C(2)–O(1)–Ta(1)	127.8(5)
O(8)–Mo(2)–O(4)#1	103.9(2)	C(1)–O(2)–Mo(1)	132.1(5)
O(5)–Mo(2)–O(4)#1	87.15(18)	C(1)–O(2)–Ta(1)	128.4(5)
O(3)–Mo(2)–O(4)#1	144.8(2)	C(3)–O(4)–Mo(2)	123.4(5)
O(4)–Mo(2)–O(4)#1	71.54(18)	C(3)–O(4)–Mo(2)#1	128.1(5)
Mo(1)–O(3)–Mo(2)	84.31(17)	C(4)–O(9)–Ta(1)	146.7(6)
Mo(2)–O(4)–Mo(2)#1	108.46(18)	C(14)–O(10)–Ta(1)	165.8(7)
Mo(2)–O(5)–Mo(1)	84.79(17)	C(18)–O(11)–Ta(1)	155.9(10)
Mo(1)–O(1)–Ta(1)	97.76(17)		

Symmetry transformations used to generate equivalent atoms: #1 $-x+2, -y+2, -z$.

symmetric oxobridges (Mo(1)–O(1) 1.926(4), Mo(1)–O(3) 1.930(4), Mo(2)–O(1) 1.910(4), Mo(2)–O(3) 1.918(4) Å in **1**, Mo(1)–O(3) = Mo(1)–O(5) 1.923(4), Mo(2)–O(3) 1.926(4), Mo(2)–O(5) 1.909(4) Å in **2** and Mo(1)–O(4) 1.915(9), Mo(1)–O(5) 1.937(11), Mo(2)–O(4) 1.932(9), Mo(2)–O(5) 1.943(9) Å in **5**) as well as the angles between these bonds lie in the range usually observed for Mo(v) alkoxides.[4,7] The major difference between the molecular structures of **1** and **2**, on one hand, and those of **5** and the homometallic complex $Mo_6O_{10}(O^iPr)_{12}$[7] on the other, lies in the presence of three bridging alkoxogroups between the terminal molybdenum atoms in the $Mo_4O_8(OR)_2$ fragments and the metal atom of the alkoxometallate ligand. This feature is, however, only a development of the trend

Table 4 Selected bond lengths (Å) and angles (°) for compound **5**

W(1)–O(8)	1.648(13)	O(1)–Mo(1)#1	2.093(10)
W(1)–O(7)	1.829(12)	Mo(2)–O(11)	1.654(10)
W(1)–O(10)	1.837(11)	Mo(2)–O(4)	1.932(9)
W(1)–O(6)	1.921(11)	Mo(2)–O(5)	1.943(9)
W(1)–O(2)	2.057(10)	Mo(2)–O(3)	2.047(9)
W(1)–O(3)	2.208(12)	Mo(2)–O(2)	2.095(11)
Mo(1)–O(9)	1.661(12)	O(1)–C(4)	1.48(2)
Mo(1)–O(4)	1.915(9)	O(2)–C(5)	1.45(2)
Mo(1)–O(5)	1.937(11)	O(3)–C(2)	1.436(18)
Mo(1)–O(1)	2.061(9)	O(6)–C(1)	1.417(19)
Mo(1)–O(1)#1	2.093(10)	O(7)–C(12)	1.33(2)
Mo(1)–Mo(2)	2.581(4)	O(10)–C(3)	1.45(2)
O(8)–W(1)–O(7)	101.8(6)	O(11)–Mo(2)–O(4)	108.9(6)
O(8)–W(1)–O(10)	97.0(5)	O(11)–Mo(2)–O(5)	107.9(5)
O(7)–W(1)–O(10)	95.2(5)	O(4)–Mo(2)–O(5)	91.5(4)
O(8)–W(1)–O(6)	97.0(5)	O(11)–Mo(2)–O(3)	103.4(5)
O(7)–W(1)–O(6)	92.7(5)	O(4)–Mo(2)–O(3)	89.6(4)
O(10)–W(1)–O(6)	162.2(5)	O(5)–Mo(2)–O(3)	146.4(4)
O(8)–W(1)–O(2)	94.6(5)	O(11)–Mo(2)–O(2)	104.2(5)
O(7)–W(1)–O(2)	163.4(5)	O(4)–Mo(2)–O(2)	145.3(4)
O(10)–W(1)–O(2)	85.4(4)	O(5)–Mo(2)–O(2)	88.2(4)
O(6)–W(1)–O(2)	82.6(4)	O(3)–Mo(2)–O(2)	72.5(4)
O(8)–W(1)–O(3)	163.2(5)	Mo(1)–O(1)–Mo(1)#1	107.2(5)
O(7)–W(1)–O(3)	93.4(5)	W(1)–O(2)–Mo(2)	104.7(4)
O(10)–W(1)–O(3)	88.5(4)	Mo(2)–O(3)–W(1)	101.1(4)
O(6)–W(1)–O(3)	75.1(4)	Mo(1)–O(4)–Mo(2)	84.3(4)
O(2)–W(1)–O(3)	70.0(4)	Mo(1)–O(5)–Mo(2)	83.4(4)
O(9)–Mo(1)–O(4)	111.9(5)	C(4)–O(1)–Mo(1)	125.1(9)
O(9)–Mo(1)–O(5)	109.7(5)	C(4)–O(1)–Mo(1)#1	127.7(9)
O(4)–Mo(1)–O(5)	92.3(4)	C(5)–O(2)–W(1)	125.7(11)
O(9)–Mo(1)–O(1)	107.1(5)	C(5)–O(2)–Mo(2)	128.5(11)
O(4)–Mo(1)–O(1)	139.5(4)	C(2)–O(3)–Mo(2)	130.9(11)
O(5)–Mo(1)–O(1)	84.9(4)	C(2)–O(3)–W(1)	122.9(10)
O(9)–Mo(1)–O(1)#1	104.0(5)	C(1)–O(6)–W(1)	132.0(12)
O(4)–Mo(1)–O(1)#1	87.1(4)	C(12)–O(7)–W(1)	148(2)
O(5)–Mo(1)–O(1)#1	143.9(4)	C(3)–O(10)–W(1)	143.8(13)
O(1)–Mo(1)–O(1)#1	72.8(5)		

Symmetry transformations used to generate equivalent atoms: #1 $-x$, $-y+1$, $-z+1$.

already present in the structure of the Mo(V,VI) complex and **5**: even there in addition to two "normal" bridges (Mo(2)–O(2) 2.095(11), Mo(2)–O(3) 2.047(9), W(1)–O(2) 2.057(10), W(1)–O(3) 2.208(12) Å in **5**) there was present a third shorter contact (Mo(2)–O(6) 2.879(12), W(1)–O(6) 1.921(11) Å to be compared with 2.880(2) and 1.919 Å respectively in $Mo_6O_{10}(O^iPr)_{12}$[7]). On the other hand, among the three bridges observed in **1** and **2**, two are shorter and more symmetric (Mo(1)–O(4) 2.081(4), Mo(1)–O(2) 2.088(3) and Nb(1)–O(4) 2.141(4), Nb(1)–O(2) 2.139(4) Å in **1**, and Mo(1)–O(1) 2.078(4), Mo(1)–O(2) 2.099(4), Ta(1)–O(1) 2.136(4), Ta(1)–O(2) 2.133(5) Å in **2**), while the third is longer and less symmetric (Mo(1)–O(11) 2.448(4), Nb(1)–O(11) 1.989(4) Å for **1**, and Mo(1)–O(6) 2.443(5), Ta(1)–O(6) 2.002(5) Å for **2**). The presence of an asymmetric contact in the system of the bridging ligands was already identified as the reason for the flexibility of the structures of this kind in solution (see below). The bond lengths and angles for the M–OR(terminal) fragments, where M = Nb, Ta, "W" are within the ranges usually observed.

The metal–oxygen core determined for the low-temperature form of **1** was found within the experimental error to be identical with that obtained for the ambient temperature modification.

The molecular structure of **3** (Figs. 4 and 5, Table 5) is the first example of a five-member ring aggregate in the chemistry of metal alkoxides. The base of the pentagon is formed by a $MoO(\mu\text{-}O)_2MoO$ fragment with a single Mo–Mo bond, which is slightly shorter than those in **1**, **2** and **5** (Mo(1)–Mo(2) 2.5730(13) Å). The lengths of both double (Mo(1)–O(12) 1.678(8), Mo(2)–O(9) 1.678(7) Å) and single Mo–O bonds forming nearly symmetrical bridges (Mo(1)–O(1) 1.915(6), Mo(1)–O(2) 1.922(7), Mo(2)–O(1) 1.918(7) and Mo(2)–O(2) 1.896(7) Å) lay within the ranges usually observed. The sides of the pentagon are formed by $Ta(O^iPr)_5$ square pyramids connected to the basal fragment by pairs of alkoxobridges (being slightly asymmetric due to a bit shorter Mo–O(R)-bridging distance 2.068–2.089(7) Å in comparison with Ta–O(R)-bridging 2.107–2.116(7) Å). The octahedral coordination of the tantalum atoms is completed by the μ-O atoms of the tetraoxomolybdate(VI)-ligand, $(\mu\text{-}O)_2MoO_2$, completing the pentagon. The latter cannot be planar if the normal bond angles should be kept for both the bridging oxygen atoms and the Mo(VI) atom. That results in the simultaneous presence of two possible orientations for the molybdate ligand—"below" and "above" the plane formed by the other four atoms (Mo(1), Mo(2), Ta(1) and Ta(2)). The distance between the central atoms in the Mo(3)–Mo(3A) is 0.881(7) Å. Both positions have equal population demonstrating the equal probability for the two orientations. The geometrical parameters for the bridging MoO_4-tetrahedra (Mo(3)O(6)O(10)O(17A)O(18A) and Mo(3A)O(6)O(10)O(17)O(18)) are in good agreement with those usually observed for such ligands.[13] However the molecule is situated in the general position and thus does not include any crystallographic symmetry element, it clearly possesses an internal symmetry plane that goes through the atoms O(1), O(2), Mo(3)/Mo(3A), O(17)/O(17A), O(18)/O(18A) as all the bond lengths and angles that should be symmetrical are identical within experimental error. This fact becomes useful in discussion of the solution structure of **3** (see below).

The structure of **6** (Fig. 6, Table 6) is built up of centrosymmetric dinuclear molecules $Ta_2(\mu\text{-}OMe)_2(O^iPr)_8$, possessing the geometry earlier predicted by Mehrotra *et al.*, *i.e.* the methoxide groups having the bridging and the isopropoxide ones the terminal function. The Ta–O bond lengths and O–Ta–O valent angles fall within the range usually observed for the tantalum alkoxides.[9]

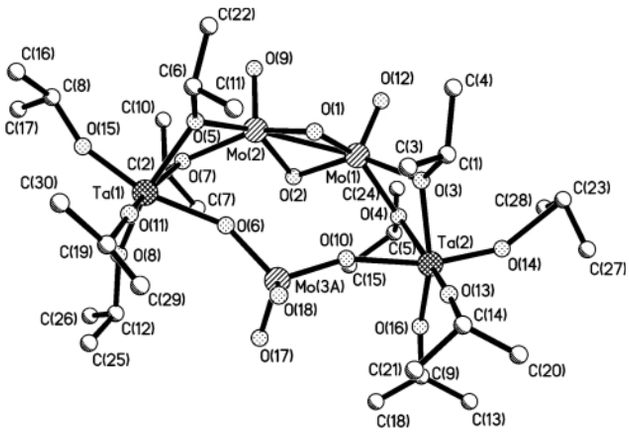

Fig. 4 The molecular structure of $Mo_3Ta_2O_8(O^iPr)_{10}$ **3**.

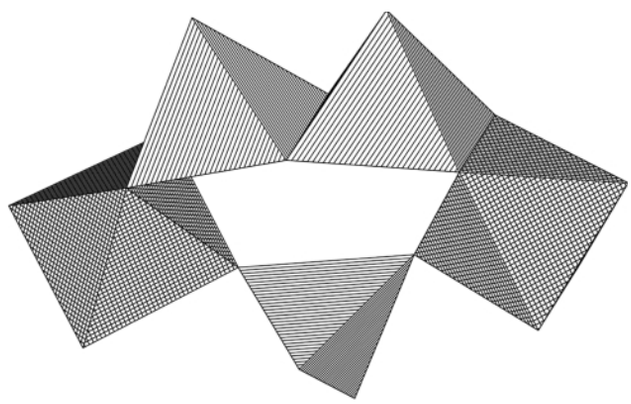

Fig. 5 The polyhedral representation of the metal–oxygen core in the molecular structure of $Mo_3Ta_2O_8(O^iPr)_{10}$ **3**.

Table 5 Selected bond lengths (Å) and angles (°) for compound **3**

Ta(1)–O(8)	1.836(9)	Mo(2)–O(1)	1.918(7)
Ta(1)–O(11)	1.846(10)	Mo(2)–O(9)	1.678(7)
Ta(1)–O(15)	1.855(8)	Mo(2)–O(7)	2.088(7)
Ta(1)–O(6)	2.062(7)	Mo(2)–O(5)	2.089(7)
Ta(1)–O(7)	2.108(7)	Mo(3)–Mo(3A)[a]	0.881(7)
Ta(1)–O(5)	2.113(8)	Mo(3)–O(17A)	1.65(3)
Ta(1)–Mo(2)	3.2106(11)	Mo(3)–O(18A)	1.74(4)
Ta(2)–O(13)	1.836(10)	Mo(3)–O(10)	1.811(8)
Ta(2)–O(16)	1.850(8)	Mo(3)–O(6)	1.847(8)
Ta(2)–O(14)	1.859(8)	Mo(3A)–O(17)	1.62(3)
Ta(2)–O(10)	2.061(7)	Mo(3A)–O(18)	1.69(2)
Ta(2)–O(3)	2.107(7)	Mo(3A)–O(6)	1.830(7)
Ta(2)–O(4)	2.116(8)	Mo(3A)–O(10)	1.831(8)
Ta(2)–Mo(1)	3.2324(11)	O(3)–C(1)	1.459(13)
Mo(1)–O(12)	1.678(8)	O(4)–C(5)	1.413(17)
Mo(1)–O(1)	1.915(6)	O(5)–C(6)	1.431(17)
Mo(1)–O(2)	1.922(7)	O(7)–C(2)	1.415(15)
Mo(1)–O(3)	2.068(7)	O(8)–C(12)	1.54(3)
Mo(1)–O(4)	2.082(7)	O(11)–C(19)	1.47(3)
Mo(1)–Mo(2)	2.5730(13)	O(15)–C(8)	1.438(18)
Mo(2)–O(2)	1.896(7)	O(13)–C(14)	1.46(3)
O(8)–Ta(1)–O(11)	99.7(5)	Mo(2)–Mo(1)–Ta(2)	133.97(4)
O(8)–Ta(1)–O(15)	97.7(4)	O(9)–Mo(2)–O(2)	108.4(4)
O(11)–Ta(1)–O(15)	98.7(4)	O(9)–Mo(2)–O(1)	109.1(4)
O(8)–Ta(1)–O(6)	91.7(4)	O(2)–Mo(2)–O(1)	92.1(3)
O(11)–Ta(1)–O(6)	92.5(3)	O(9)–Mo(2)–O(7)	100.3(4)
O(15)–Ta(1)–O(6)	163.9(4)	O(2)–Mo(2)–O(7)	90.6(3)
O(8)–Ta(1)–O(7)	94.0(4)	O(1)–Mo(2)–O(7)	147.9(3)
O(11)–Ta(1)–O(7)	162.5(4)	O(9)–Mo(2)–O(5)	102.3(3)
O(6)–Ta(1)–O(5)	76.9(3)	O(2)–Mo(2)–O(5)	147.1(3)
O(7)–Ta(1)–O(5)	71.4(3)	O(1)–Mo(2)–O(5)	88.8(3)
O(13)–Ta(2)–O(16)	100.8(5)	O(7)–Mo(2)–O(5)	72.2(3)
O(13)–Ta(2)–O(14)	97.1(5)	Mo(1)–Mo(2)–Ta(1)	133.96(4)
O(16)–Ta(2)–O(14)	98.1(4)	O(17A)–Mo(3)–O(18A)	108(3)
O(13)–Ta(2)–O(10)	92.0(4)	O(10)–Mo(3)–O(6)	109.2(4)
O(16)–Ta(2)–O(10)	92.3(3)	O(17A)–Mo(3)–O(6)	113.3(9)
O(14)–Ta(2)–O(10)	164.6(4)	O(18A)–Mo(3)–O(6)	103(2)
O(13)–Ta(2)–O(3)	94.6(4)	O(17A)–Mo(3)–O(10)	115.5(10)
O(16)–Ta(2)–O(3)	161.4(3)	O(18A)–Mo(3)–O(10)	107(2)
O(14)–Ta(2)–O(3)	90.2(3)	O(17)–Mo(3A)–O(18)	106.5(17)
O(10)–Ta(2)–O(4)	77.0(3)	O(17)–Mo(3A)–O(6)	109.6(15)
O(3)–Ta(2)–O(4)	71.3(3)	O(18)–Mo(3A)–O(6)	111.5(10)
O(12)–Mo(1)–O(1)	108.3(4)	O(17)–Mo(3A)–O(10)	108.8(14)
O(12)–Mo(1)–O(2)	107.6(4)	O(18)–Mo(3A)–O(10)	111.4(9)
O(1)–Mo(1)–O(2)	91.4(3)	O(6)–Mo(3A)–O(10)	109.1(4)
O(12)–Mo(1)–O(3)	104.9(4)	Mo(1)–O(1)–Mo(2)	84.3(3)
O(1)–Mo(1)–O(3)	88.6(3)	Mo(2)–O(2)–Mo(1)	84.8(3)
O(2)–Mo(1)–O(3)	145.8(3)	Mo(1)–O(3)–Ta(2)	101.5(3)
O(12)–Mo(1)–O(4)	102.5(4)	Mo(1)–O(4)–Ta(2)	100.7(3)
O(1)–Mo(1)–O(4)	147.2(3)	Mo(2)–O(5)–Ta(1)	99.7(3)
O(2)–Mo(1)–O(4)	89.8(3)	Mo(3)–O(6)–Ta(1)	150.9(5)
O(3)–Mo(1)–O(4)	72.7(3)	Mo(2)–O(7)–Ta(1)	99.8(3)

[a] The disordered dioxomolybdenyl fragments are Mo(3A)O(17)O(18) and Mo(3)O(17A)O(18A).

Isolation and solution structure of the reaction products

Thermal reduction of molybdenum(VI) alkoxides and formation of molybdenum(V) bimetallic derivatives. Taking into account the spontaneous and practically complete decomposition of $MoO(O^iPr)_4$ on storage with formation of a mixed-valence derivative:[8,14]

$$6MoO(O^iPr)_4 \rightarrow Mo_6O_{10}(O^iPr)_{12} + 2(CH_3)_2CO + 2^iPrOH + 4(^iPr)_2O \quad (1)$$

we expected the reaction between the molybdenum isopropoxide and the isopropoxides of niobium and tantalum to occur at room temperature. The color of the mixed-metal solutions remained, however, unchanged in time in contrast to the solutions of pure molybdenum alkoxide. That was indicative of an interaction between the components, but their NMR spectra remained unchanged in the mixed-metal solutions and the pure

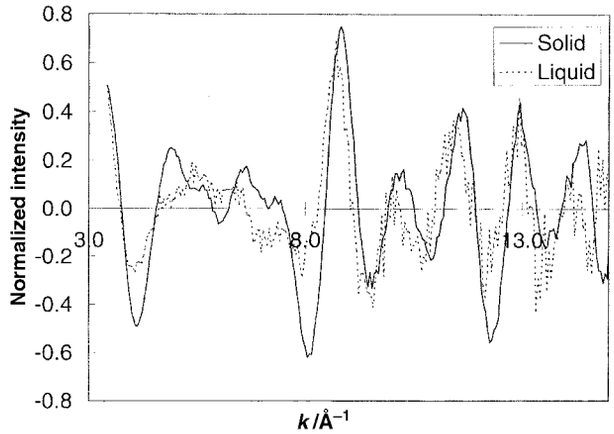

Fig. 6 Experimental EXAFS data on Mo for **2** in the solid state (——) and in solution (– – –).

Table 6 Selected bond distances and angles in the structure of **6**

Ta(1)–O(3)	1.815(8)	O(1)–Ta(1)#1	2.122(5)
Ta(1)–O(2)	1.838(7)	O(2)–C(4)	1.344(16)
Ta(1)–O(5)	1.857(7)	O(3)–C(5)	1.405(19)
Ta(1)–O(4)	1.895(6)	O(4)–C(2)	1.269(16)
Ta(1)–O(1)	2.114(5)	O(5)–C(3)	1.282(16)
Ta(1)–O(1)#1	2.122(5)	C(3)–C(31)	1.39(2)
O(1)–C(1)	1.390(10)	C(3)–C(32)	1.43(2)
O(3)–Ta(1)–O(2)	177.7(3)	O(3)–Ta(1)–O(1)#1	90.6(2)
O(3)–Ta(1)–O(5)	90.4(3)	O(2)–Ta(1)–O(1)#1	87.6(2)
O(2)–Ta(1)–O(5)	91.8(3)	O(5)–Ta(1)–O(1)#1	160.8(2)
O(3)–Ta(1)–O(4)	89.3(3)	O(4)–Ta(1)–O(1)#1	94.1(3)
O(2)–Ta(1)–O(4)	89.4(3)	O(1)–Ta(1)–O(1)#1	69.8(2)
O(5)–Ta(1)–O(4)	105.1(3)	C(1)–O(1)–Ta(1)	125.3(6)
O(3)–Ta(1)–O(1)	88.6(2)	C(1)–O(1)–Ta(1)#1	122.2(6)
O(2)–Ta(1)–O(1)	92.1(2)	Ta(1)–O(1)–Ta(1)#1	110.2(6)
O(5)–Ta(1)–O(1)	91.1(2)	C(4)–O(2)–Ta(1)	160.7(10)
O(4)–Ta(1)–O(1)	163.7(2)	C(5)–O(3)–Ta(1)	163.0(10)

Symmetry transformations used to generate equivalent atoms: #1 $-x + 1, -y, -z$.

$MoO(O^iPr)_4$ could even be partially separated by crystallization at low temperatures (−20 to −30 °C).

The heating of the solutions under reflux led to rather quick, while not immediate, color change from yellow, characteristic of Mo(VI) monooxoderivatives,[15] to orange-red or orange-brown typical for Mo(V) alkoxides.[4,7] The solid state molecular structures of the products that could be easily isolated by crystallization on cooling turned out to be very closely related to that of $Mo_6O_{10}(O^iPr)_{12}$. It can thus be postulated that they originate from the complexation of $[MoO_2(O^iPr)]_4$ formed on thermal decomposition of molybdenum(VI) oxoisopropoxide as a very strong Lewis acid with the alkoxides of Nb or Ta as weak Lewis bases. The reaction pathway in this case is similar to that for the interaction of pyridine with $MoO(O^iPr)_4$: the latter on one side remains unchanged in the presence of even traces of C_5H_5N[8] and, on the other side, the addition of pyridine to the toluene solutions of $Mo_6O_{10}(O^iPr)_{12}$ (formed on decomposition of $MoO(O^iPr)_4$), which leads to the precipitation of $[MoO_2(O^iPr)(py)]_4$.[7] It is possible then to conclude that the presence of Lewis bases (donor ligands) decreases the electron deficiency of the Mo(VI)-center and thus its strength as the oxidant; even in the cases when no stable complex is formed. On the other hand they win against residual $MoO(O^iPr)_4$ (quite a weak Lewis base) in the competition for the electron-deficient Mo(V) dioxoalkoxide centers formed after the partial thermal decomposition. These reactions occur easily and quickly due to the rather high fluxionality of the structure of $Mo_6O_{10}(O^iPr)_{12}$ in solution.[7] It is interesting to point out that the structures of **1** and **2** also are rather fluxional in solution. Only one signal for both methyl and methyne protons is observed in their ^1H NMR

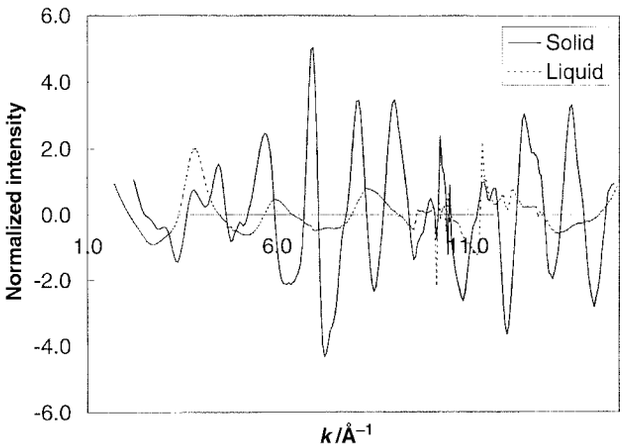

Fig. 7 Experimental EXAFS data on Ta for **2** in the solid state (——) and in solution (– – –).

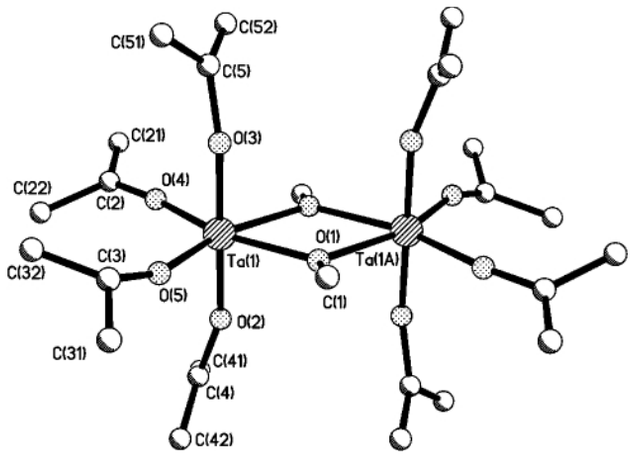

Fig. 8 The molecular structure of $Ta_2(OMe)_2(O^iPr)_8$ **6**.

spectra at room temperature. It becomes split at low temperatures (−50 °C) for both of them but in a different way: the single signal for methine protons (septet) in the spectrum of **1** gives three broad unresolved signals with 4:2:1 ratio of integral intensities indicating presumably the presence of only two alkoxide bridges between Mo and Nb in the solution structure (that can thus be formulated as $[(RO)_4Nb(\mu\text{-}OR)_2MoO(\mu\text{-}O)_2MoO(\mu\text{-}OR)]_2$. The single C*H*-signal in the spectrum of **2** is first split into two signals with a 4:3 integral ratio and on further cooling into three with a 1:3:3 integral ratio indicative of the same kind of structure as that observed for the solid phase. The EXAFS spectral data obtained demonstrate that only very slight changes occur in the arrangement of the Mo-atoms on transition of **2** from the solid phase into a toluene solution (see Fig. 6). A probable structural model based on Mo in a square pyramidal coordination (Mo=O apical ≈1.7 Å, 4 Mo–O equatorial ≈1.9 Å) also introducing an additional Mo–Mo contact with bond length of ≈2.6 Å adequately describes the EXAFS spectrum observed. The coordination of Ta atoms in **2** was in contrast definitely a subject for rather considerable changes on dissolution (see Fig. 7). The best model for the description of the liquid EXAFS spectrum is an octahedral arrangement of the oxygen atoms (O_h symmetry, three contacts at 1.8 and three at 2.0 Å). The presence of the Mo atoms at quite a short distance (3.2 Å according to the X-ray single crystal structure) does not improve the structural model significantly. The changes on dissolution appear to be connected with the shortening of Ta–O distances and maybe even with the decrease in coordination number. These data propose that while the central $[MoO_2(O^iPr)]_4$ core is essentially preserved in solution at room temperature, it either has much weaker contacts with the terminal $Ta(O^iPr)_5$ groups or even allows them to dissociate partially as monomers of tantalum isopropoxide.

The specific feature in the formation of **5** is that $WO(O^iPr)_4$ is a stronger Lewis acid than $MoO(O^iPr)_4$, which it should replace in the structure of $Mo_6O_{10}(O^iPr)_{12}$, and as a result acts as a weaker Lewis base. The molecules of the reaction product $Mo_4W_2O_{10}(O^iPr)_{12}$ have the geometrical parameters nearly exactly identical to those of the homometallic complex and it results in the formation of a solid solution between them. The average tungsten content in the samples increases with increasing time of reflux, but at the same time the yield of the crystalline product decreases. The latter apparently occurs due to the loss of $WO(O^iPr)_4$ because of its thermal decomposition into $WO_2(O^iPr)_2$ *via* ether elimination described earlier in the literature.[15]

We have made attempts at the preparation of the analogous derivatives using $Ti(O^iPr)_4$ and $Al(O^iPr)_3$ as heteroligands. We could, however, observe the precipitation of pure homometallic derivative, $Mo_6O_{10}(O^iPr)_{12}$, in the former case, while no crystalline product could be isolated from the solutions containing aluminium isopropoxide. The aluminium alkoxides are known for their tendency to form various stable oxocomplexes and therefore the redistribution of the oxoligands preventing crystallization might be suspected in the latter case.

Formation of the decomposition products of molybdenum(v) bimetallic alkoxides. The bimetallic molybdenum(v,vi) alkoxide **3**, $Mo_3Ta_2O_8(O^iPr)_{10}$, was originally isolated as the major product of the interaction of "tantalum isopropoxide" prepared from $Ta(OMe)_5$ *via* an alcohol interchange reaction. The latter led to $[Ta(O^iPr)_4(OMe)]_2$ **6**, as it was earlier described in the literature,[16] and we really observed one fifth of the methoxide groups to be conserved in the product according to NMR spectroscopic data. We were even able to isolate the single crystals of **6** (see Fig. 8) on cooling to −30 °C from the solutions analogous to those from which **3** was obtained but not subjected to heat treatment. The presence of the methoxide ligands in the system evidently changed the reaction pathway that should otherwise have been identical to that of the reaction (1):

$$4MoO(O^iPr)_4 + 2Ta(O^iPr)_5 \rightarrow Mo_4Ta_2O_8(O^iPr)_{14} + 2(CH_3)_2CO + 2^iPrOH + 4(^iPr)_2O \quad (2)$$

The further interaction of ^{i}PrOH with acetone is sterically hindered but in boiling toluene it would participate in the equilibrium with the methoxide ligands giving rise to MeOH, which in its turn was shown to react with acetone in the presence of molybdenum(vi) alkoxides:[14]

$$(CH_3)_2CO + 2MeOH \rightarrow (CH_3)_2C(OMe)_2 + H_2O \quad (3)$$

$$3MoO(O^iPr)_4 + Ta_2(OMe)_2(O^iPr)_8 \rightarrow Mo_3Ta_2O_8(O^iPr)_{10} + (CH_3)_2C(OMe)_2 + {}^iPrOH + 4(^iPr)_2O \quad (4)$$

The molecules of water formally released in this reaction lead to hydrolysis and formation of the more substituted oxocomplexes. This latter fact explains the formation of a product containing the oxomolybdate ligand in its molecular structure when a precursor contaminated with methoxide is applied. The formation of **3** as the first decomposition product was also observed in the NMR spectra of the samples of **2** subjected to oxidation by dry oxygen. The structure of **3** is conserved in solution and apparently remains quite rigid as the ^{1}H NMR spectra display two well defined signals for both CH and CH_3 fragments in a 3:2 ratio corresponding to the ratio of the number of terminal to the number of bridging groups (6:4) in the molecule of **3**. The pairs of bridging and triads of terminal

groups were not related in the structure of **3** by the crystallographic elements of symmetry, but the geometrical parameters of the molecule definitely indicated their equivalence to each other. The ^{13}C spectrum of **3** is more complicated as these signals might be more sensitive to the arrangement of the isopropyl radicals with respect to each other and the metal–oxygen core. It is interesting to note that the ^{17}O spectrum appears to be in good agreement with the molecular structure of **3**: it contains both the signals corresponding to the oxygen atoms bound to square pyramidal coordinated Mo(V) atoms at 578, 552 (supposedly corresponding to Mo(V)-μ-O-Mo(V) fragments) and 46 ppm (supposedly Mo(V)=O) see ref. 8 and those bound to Mo(VI) atoms at 872.8, 880.3, 895.5 and 903.6 ppm (four bonds in the MoO_4^{2-} bridging ligand, compare 862–894 ppm for Mo=O bonds in Mo(VI) alkoxides[7]) thus demonstrating the simultaneous presence and spatial separation of different oxidation states for Mo atoms.

On longer storage in contact with dry oxygen in the flasks connected to the atmosphere *via* a column filled with dry molecular sieves, the orange color of solutions of **2** and **3**, corresponding to the presence of Mo(V)–Mo(V) fragments, disappears completely and on slow evaporation of the solvent a precipitation of colorless rectangular crystals of **4** commences. In both cases the crystal identity was proved by the determination of unit cell parameters for a statistically representative number of single crystals. The yields of compound **4** are always minor and it appears quite reasonable as its composition deviates rather noticeably from the average one in the system. The other reason for the low yields of **4** might be the extremely high solubility of this compound in hydrocarbon solvents. It should be mentioned that it has been almost impossible to obtain **4** *via* partial hydrolysis of hydrocarbon solutions containing Mo and Ta isopropoxides in a 1 : 1 molar ratio. The reason for this failure might be that the formation of bimetallic species in this case occurs *via* a Lewis acid–base interaction mechanism and the latter would be hindered by the ^{i}PrOH released on hydrolysis as it is a much stronger Lewis base than the alkoxides in question. The structure of **4** is presumably preserved in solution in hydrocarbons as the NMR spectra obtained in toluene display only one very well defined signal for both methyne and methyl protons (all the isopropoxide groups in the solid state structure of **4** are related by the crystallographic elements of symmetry), while the dissociation in solution would supposedly lead to the appearance of several different signals. It is important to note that the appearance of first **3** and then **4** on oxidation of **2** by dry oxygen was also traced in the NMR spectra.

Acknowledgements

We express our sincerest gratitude to Dr Gunnar Westin and Mrs Åsa Ekstrand for help with EDS and to Dr Corine Sandström and Dr Rolf Andersson for assistance with the NMR measurements and to the Swedish Council for Natural Science Research for financial support of this work.

References

1 C. Limberg, S. Parsons, A. J. Downs and D. J. Watkin, *J. Chem. Soc.*, *Dalton Trans.*, 1994, 1169.
2 H. Funk, M. Hasselbarth and F. Schmeil, *Z. Anorg. Allg. Chem.*, 1962, **318**, 318.
3 M. Yu. Antipin, Yu. Struchkov, A. Shilov and A. Shilova, *Gazz. Chim. Ital.*, 1993, **123**, 265.
4 V. G. Kessler, A. N. Panov, N. Ya. Turova, Z. A. Starikova, A. I. Yanovsky, F. M. Dolgushin, A. P. Pisarevsky and Yu. T. Struchkov, *J. Chem. Soc.*, *Dalton Trans.*, 1998, 21.
5 A. Johansson and V. G. Kessler, *Polyhedron*, submitted.
6 M. H. Chisholm, C. C. Kirkpatrick and J. C. Huffman, *Inorg. Chem.*, 1981, **20**, 871.
7 M. H. Chisholm, J. C. Huffman, K. Folting and C. C. Kirkpatrick, *Inorg. Chem.*, 1984, **23**, 1021.
8 V. G. Kessler, A. V. Shevelkov and L. A. Bengtsson-Kloo, *Polyhedron*, 1998, **17**, 965.
9 N. Ya. Turova, A. V. Korolev, D. E. Tcheboukov and A. I. Belokon, *Polyhedron*, 1996, **15**, 3869.
10 E. P. Turevskaya, N. Ya. Turova, A. V. Korolev, A. I. Yanovsky and Yu. T. Struchkov, *Polyhedron*, 1995, **14**, 1531.
11 SHELXTL 5.3 Reference Manual, Bruker AXS, 1997.
12 B. K. Teo, *EXAFS: Basic Principles and Data Analysis*, *Inorganic Chemistry Concepts*, vol. 9, Springer, Berlin, 1986.
13 M. I. Khan and J. Zubieta, *Progr. Inorg. Chem.*, 1995, **43**, 1.
14 V. G. Kessler, K. V. Nikitin and A. I. Belokon, *Polyhedron*, 1998, **17**, 2309.
15 N. Ya. Turova, V. G. Kessler and S. I. Kucheiko, *Polyhedron*, 1991, **10**, 2617.
16 D. C. Bradley, R. C. Mehrotra and D. Gaur, *Metal Alkoxides*, Academic Press, London, 1978.

Paper a907720k